Progress In Electromagnetics Research B, Vol. 23, 293–309, 2010

COMPARISON OF TWO TYPES OF DUAL LAYER GENERATOR IN FIELD ASSISTED MODE UTILIZING 3D-FEM AND EXPERIMENTAL VERIFICATION

E. Afjei and H. Torkaman

Department of Electrical and Computer Engineering
Shahid Beheshti University, G.C.
Tehran, Iran

Abstract—This paper presents the comparison results between two new generator configurations. These generator units are namely a field assisted switched reluctance generator (SRG) and a brushless dc (BLDC) generator. No permanent magnets are used in either unit. The field assisted SR generator consists of two magnetically dependent stator and rotor sets (layers), where each stator set includes twelve salient poles with windings wrapped around them, while the rotor comprises of eight salient poles without any winding or permanent magnet. There is a stationary reel, which has the field coil wrapped around it and is placed between the two-stator sets. The BLDC generator is also made up of two magnetically dependent stator and rotor sets, but each stator set includes nine salient poles with windings wrapped around them while, the rotor comprises of six salient poles without any windings or permanent magnets. There is also a stationary reel between the two layers to produce the magnetic field through the motor assembly. This magnetic field travels through a guide to the rotor then the stator and finally completes its path via the generator housing. The generator phase windings for each layer are connect such that all the stator poles in that set can have either north or south pole configuration while the stator poles in the other layer have the opposite pole arrangement. This type of connection can be used in motoring mode as well. To evaluate the performance of the generators, two types of analysis, namely, numerical technique and experimental study have been utilized. In the numerical analysis, three dimensional finite element analysis is employed, whereas in the experimental study, proto-types have been built and tested.

Received 8 June 2010, Accepted 19 July 2010, Scheduled 25 July 2010
Corresponding author: H. Torkaman (h_torkaman@sbu.ac.ir).

1. INTRODUCTION

Nowadays, various parameters such as variable load flexibility, high reliability, low investment cost and maintenance, small transmission loss leads to have more attention in the area of distributed power generation systems. As a result of several researches to achieve this purpose, well-developed technologies in the area of reluctance and brushless dc generators have now evolved. Whereas, both generator types offer a number of advantages and supply proportionate to applications demands [1, 2].

Moreover, with the quick and wide development of the control technologies and power electronic instruments, the brushless electric machines are replacing with the brush electric machines, and also mechanical switches are replaced with much faster and more reliable solid state electronic switches [3–5]. Consequently, the switched reluctance and brushless dc generators have been developed for various shapes and sizes in different power ratings and used in industry [6, 7].

The reluctance machine has begun to realize its potential in the new era of power electronics and computer-aided electromagnetic design. The machine development has matured to the point that its impact is now evident in the industry. The types of reluctance machines available in the marketplace today are primarily of the regular cylindrical geometry although the disc and multi layer geometries have been proposed in limited use [8, 9]. SR Generator (SRG) is also an attractive solution for worldwide increasing demands for electrical energy. It is low cost, fault tolerant with a rugged structure and operates with high efficiency over a wide speed range. The SRG have been utilized for some applications like starter/generator for gas turbine of aircrafts [10, 11] wind power generator [12, 13] and as an alternator for automotive applications [14, 15]. These machines provide several advantages including simplicity in construction, cooling, geometric versatility, durability, and higher permissible rotor temperature.

The BLDC machines have gained popularity due to the development of high flux density and reliable and permanent magnets. BLDCMs are used in industries for different applications such as, automotive, aerospace, home appliances, and many industrial equipment and instrumentation [16, 17]. The construction of modern BLDC machines is very similar to the ac machine, known as the permanent magnet synchronous machine. Out of these, 3-phase machines are the most popular and widely used. The stator of a BLDCM consists of stacked steel laminations with windings placed in the slots that are axially cut along the inner periphery or around

stator salient poles. The rotor is made of permanent magnet and can vary from two to eight pole pairs with alternate north (N) and south (S) poles.

The standard BLDC generator lacks field control due to use of permanent magnet in the rotor assembly. The output voltage can be controlled by either variation in generator speed or use of some kind of drive circuit to hold the output voltage at a desirable level for different speeds. A standard SRG can only produce power during the decreasing phase inductance profile which limits its output power production.

The new generators use a field assisted scheme to produce the magnetic flux through the machine assembly. It also does not use any kinds of brushes for the stationary field coil placed between the two stator sets. The current flows into the coil by simply connecting the field terminals to a dc voltage source, and it can be controlled easily to produce the desired output voltage at almost any speed. The current through the field can be reduced to zero in case of any malfunctioning of the drive circuit in order to protect the generator load from high voltage production at high speeds.

In this paper, the comparison results of a new brushless DC generator, with a switched reluctance generator in their new configurations have been studied. These generators are good candidates for hybrid vehicles applications and wind energy conversion systems in low voltage applications. The proposed generators are constructed with two layers and a field assisted unit. The design and optimization of the machines for comparative study was performed with the aid of a three dimensional finite element magnetic field package.

This paper is organized as follows: Section 2 briefly explains the double layer machines design and calculated geometrical parameters in both of them. The three dimensional finite element results of the generators electromagnetic profiles are obtained and compared in Section 3. Section 4 contains the discussion about generated voltage in machines and Section 5 includes the physical assembly of the two machines as well as the experimental results obtained from the new dual layer switched reluctance and brushless dc generators, and followed by conclusions in Section 6.

2. THE DESIGN FEATURES OF PROPOSED DUAL LAYER MACHINES

In design procedure of the generators, for achieving maximum output voltage as well as power for a certain machine volume, a new construction in their geometries are considered. The generator

configurations for brushless dc and switched reluctance units are modified and designed based on having double layers of the stator/rotor and a stationary field assisted coil placed between them. These modifications caused significant improvements in both generator units which makes them distinct from other types of generators. These configurations consist of two layers and a field coil which produce South Pole in one layer and the North Pole in the other layer. In addition, due to existence of a field assisted coil between the two layers an independent field is produced in the generator units, which can produce higher output power than a standard self excited generator. The design details are briefly explained below.

2.1. Dual Layer dc Generatr (DLDCG)

The brushless generator consists of two magnetically dependent stator and rotor layers (sets), where each stator set includes nine salient poles with windings wrapped around them while, the rotor comprises of six salient poles. Every stator and rotor pole arc is about 30°. The two layers are exactly symmetrical with respect to a plane perpendicular to the middle of the generator shaft. This is a three phase generator, therefore, three coil windings from one layer is connected in series with the other three coil windings in the other layer. These coils together make one of the generator phases.

There is a stationary reel, which has the field coils wrapped around it and is placed between the two-stator sets. This reel has a rotating cylindrical core, which guides the magnetic field. The magnetic flux produced by the coils travels through the guide and the shaft to the rotor and then to the stator poles, and finally closes itself through the generator housing. Therefore, one set of the rotor poles has magnetically North Pole while the other set is magnetically South Pole configuration. In this generator, the magnetic field has been induced to the rotor without using any brushes to inject the current into the field winding.

In order to get a better view of the generator configurations, the complete generator assembly without coils winding is shown in Fig. 1.

The proposed DLDC generator dimensions are listed in Table 1.

2.2. Dual Layer Switched Reluctance Generator (DLSRG)

The switched reluctance generator consists of two magnetically dependent stator and rotor layers, where each stator set includes twelve salient poles with windings wrapped around them while, the rotor comprises of eight salient poles. Every stator and rotor pole arcs are 14° and 16°, respectively. The two layers are exactly symmetrical with

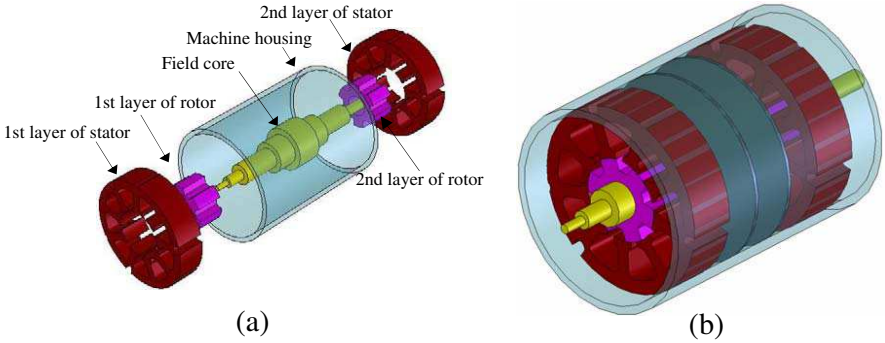

Figure 1. The DLDC generator; (a) different parts, (b) complete assembly (without coil windings).

Table 1. DLDC generator dimensions.

Parameter	Value
Stator core outer diameter	78 mm
Stator core inner diameter	68 mm
Rotor core outer diameter	35.5 mm
Length of air gap	0.25 mm
Shaft diameter	15 mm
Rotor pole arc	30°
Stator pole arc	30°
Number of turns per stator pole	120
Number of turns in assistant field	300

respect to a plane perpendicular to the middle of the generator shaft. This is a three phase generator, therefore, four coil windings from one layer is connected in series with the other four coil windings in the other layer. The coil windings in each layer are such that the stator poles gain either North or South Pole configuration for the generator mode. In the machine operation each layer can operate independently, in series or parallel with each other. In another words, each layer consist of a twelve by eight cylindrical switched reluctance generator configuration sharing common shaft and can be connected to each other in three possible ways. There is a stationary reel, which has the field coils wrapped around it and is placed between the two-stator sets. This reel has a rotating cylindrical core, which guides the magnetic field. The magnetic flux produced by the coils travels through the guide and the

generator shaft to the rotor and then to the stator poles, and finally closes itself through the generator housing. Therefore, one set of rotor poles is magnetically north and the other set is magnetically south. In this generator, the magnetic field has been induced in the rotor without using any brushes to inject current in to the field winding.

For a better illustration of the proposed generator configurations, the complete assembly without coils winding is presented in Fig. 2.

The DLSR generator specifications calculated for the study is shown in Table 2.

It must be pointed out that the machines have different diameters but they have the same volume and the same amount of iron in stators and rotors are used. This is note worthy to mention that these generators can operate in two modes of operation namely; filed

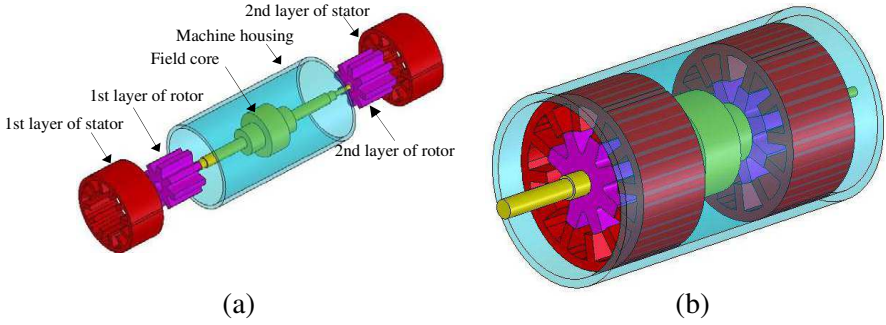

Figure 2. The DLSR generator; (a) different parts, (b) complete assembly (without coil windings).

Table 2. DLSR generator dimensions.

Parameter	Value
Stator core outer diameter	72 mm
Stator core inner diameter	62 mm
Rotor core outer diameter	41.5 mm
Length of air gap	0.25 mm
Shaft diameter	15 mm
Rotor pole arc	16°
Stator pole arc	14°
Number of turns per stator pole	100
Number of turns in assistant field	300

assisted mode and self excited mode. In this study field assisted mode is considered for the comparative study in this paper. Two types of analysis namely numerical and experimental have been performed.

3. COMPARISON OF ELECTROMAGNETIC PROPERTIES

To properly evaluate the generator design and performance, a reliable model is required [18–20]. Finite element analysis (FEA) is being used to determine the magnetic field distribution in and around the generator [21, 22]. In order to present the operation of the generator and to determine the main profiles and parameters at different positions of the rotor, the field solutions are obtained. The three dimensional field analysis has been performed using a Magnet CAD package [23] to consider the end effects and axial fringing fields effect for simulating reliable model which is based on the T-Ω technique.

In the finite element analysis, second order triangular elements with dense meshes at places where the variation of fields are greater have been used.

In this analysis, the usual assumptions such as the magnetic field outside of an air box in which the generator is placed, is considered to be zero. The comparison results for 9/6 DLDCG and 12/8 DLSRG including magnetic flux density, flux-linkages, terminal inductance per phase, mutual inductances and produced voltage for various excitation in one complete rotor rotation are obtained and discussed below.

3.1. Magnetic Flux Density

The design of the generator becomes complicated due to complex geometry and material saturation. Moreover an accurate knowledge of the flux distribution inside the generator for different excitation currents and rotor positions are essential for the prediction of generator performance. These generators can be highly saturated under normal operating conditions. Fig. 3 shows the magnetic flux density arrows for fully-aligned case when the generators operates in the field assisted mode, which produce north pole in one layer and south pole in the opposite layer. Hence for proper operation of the generator, the two layers should be working simultaneously. The field current is considered to be at 0.5 A for this study.

As shown in Fig. 3, the majority of flux distribution is concentrated in aligned stator and corresponding rotor poles. The amplitude of magnetic flux densities in aligned stator poles is 0.95 and

1.42 Tesla for DLDCG and DLSRG, respectively. These values show the DLSR generator operates in nonlinear or saturation region.

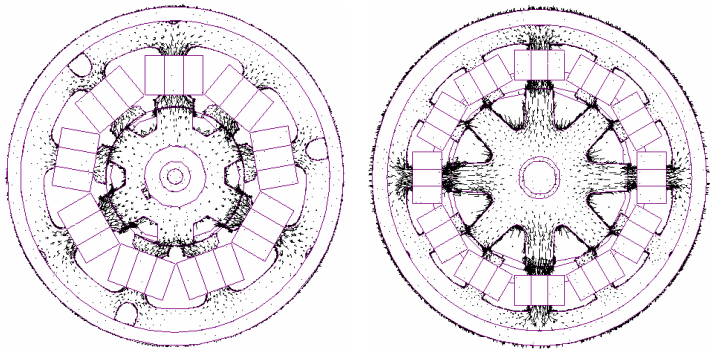

Figure 3. The magnetic flux density for fully-aligned cases in: (a) DLDCG, (b) DLSRG.

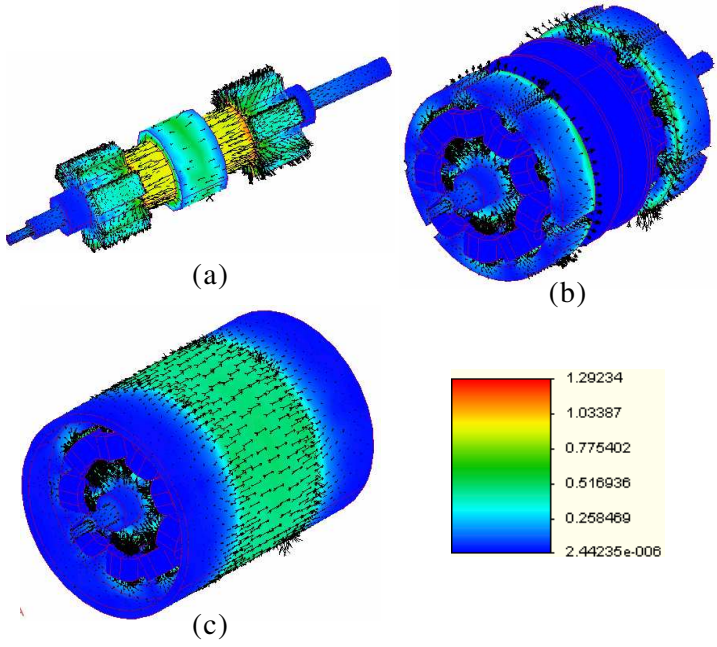

Figure 4. The magnetic flux density for half-aligned cases in DLDCG: (a) without stators and housing, (b) without housing, (c) complete assembly.

The plots of magnetic flux density for the generators in half-aligned case for different generators parts are shown in Fig. 4 and Fig. 5.

Figures 4 and 5 show the aligned corner of rotor and stator poles are in saturation and maximum magnetic flux density is about 1.02 Tesla in reluctance generator. Also, the maximum magnetic flux density in dc generator is about 0.95 Tesla at some small local points on the very tip of the stator pole. For assessing the generators operation, the assisted field is excited under different current amplitudes (I_f) in both of machines. Maximum flux density in stator pole for various current excitations in fully alignment (B_{fa}) and half alignment (B_{ha}) positions are listed in Table 3.

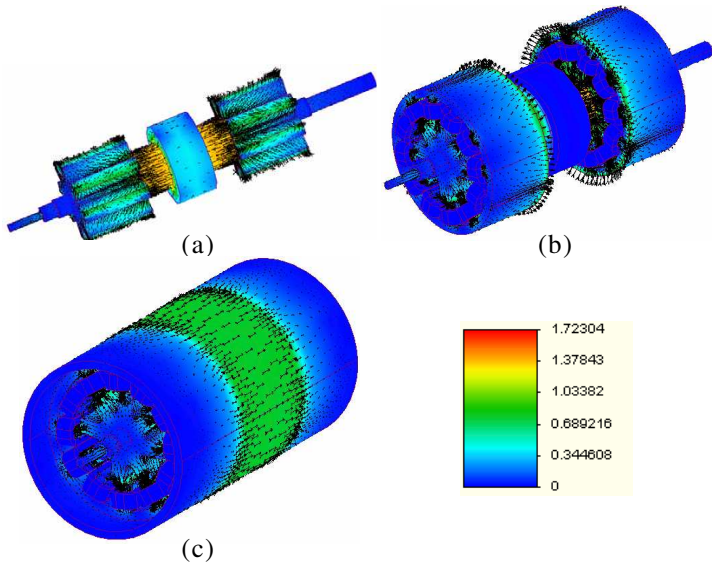

Figure 5. The magnetic flux density for half-aligned cases in DLSRG: (a) without stators and housing, (b) without housing, (c) complete assembly.

Table 3. Maximum flux density in stator pole.

Machine Type	DLDCG			DLSRG		
I_f (A)	0.25	0.5	0.75	0.25	0.5	0.75
B_{fa} (T)	0.40	0.79	0.99	0.71	1.02	1.09
B_{ha} (T)	0.56	0.95	1.18	1.07	1.42	1.50

As depicted in Table 3, with an increase in field current the amplitude of flux densities in fully and half alignment rotor positions are increased in both generators. On the other side, the flux density of DLSRG in fully alignment has 43%, 22% and 9% higher amplitude than DLDCG under 0.25, 0.5 and 0.75 A field current, respectively. In addition, these values go up to 47%, 33% and 21% when the machine is in half alignment rotor position which causes more magnetic force between rotor and stator poles. The differences between flux densities in both machines are due to their geometries in terms of the number of stator and rotor poles. Since the numbers of poles in fully aligned position as well as the amount of overlapping in SR generator are more than the dc generator, then the flux magnitude is higher in SRG. In other words, complete aligned position in dc generator accompanied by more mutual flux due to stator poles configuration compared to SR generator. From another point of view, the higher flux amplitude of reluctance generator can be disadvantageous when the asymmetrically disturbance occurs because that leads the generator to face with more noise and vibration.

3.2. Flux Linkage and Inductance

In this study, the analysis includes a 360 degree rotation of the rotor to analyze the generators behaviors at the different rotor positions. Due to symmetrical shape of the stator/rotor assembly, the rotor movement from fully aligned to unaligned position is considered (phase A) for evaluating the performance of the generators. Fig. 6 shows the flux linkage for phase A in DLDCG that includes 6 series coils from two stator assembly.

Figure 7 illustrates the flux linkage from phase A in DLSRG which includes 8 series coils from two stator layers. The mutual inductance has been defined as the ratio of each phase flux linkage to the exciting current of the assisted field (Eq. (9)). Therefore, the variation of mutual inductance is proportional to variation of flux linkage when the current is considered to be constant.

$$L = \lambda(\theta)/I_f \tag{1}$$

As shown in Fig. 6 and Fig. 7, the amplitude of flux linkage as well as the phase inductance will go up in both machines with raising the field current. As shown in these figures, the maximum amplitude of terminal inductance in DLSR generator is 1.9, 1.6 and 1.3 times higher than those of inductance amplitude in DLDC generator, with 0.25, 0.5 and 0.75 A of field current, respectively.

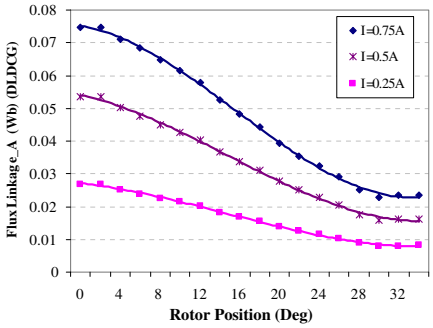

Figure 6. The flux linkage for phase A in DLDCG.

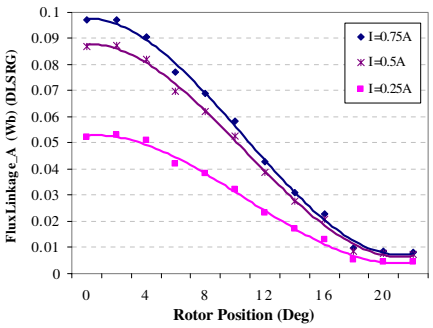

Figure 7. The flux linkage for phase A in DLSRG.

4. COMPARISON OF VOLTAGE PRODUCTION

As seen from Fig. 1 and Fig. 2, the DLDCG has nine stator poles as well as six rotor poles, while DLSRG has twelve stator poles as well as eight rotor poles which will be engaged in the voltage production mechanism. In this analysis the produced voltages in proposed generators are obtained based on Faraday's law of induction (Eq. (2)) which explains that the induced voltage (V), in the generator depends on the number of turns (N) and the time derivative of magnetic flux. It is expressed as follow,

$$V = -N\frac{d\varphi}{dt} = -N\frac{d\varphi}{d\theta}\cdot\frac{d\theta}{dt} = -N\frac{d\varphi}{d\theta}\omega \tag{2}$$

In order to estimate the shape of the generated voltage, the obtained simulated flux linkage data are estimated by a fourth order equation. The voltage produced in each coil is computed using Eq. (2). Coils 1,2,3 from 1st layer, and coils 4,5,6 from 2nd layer are in series and they are belong to phase A then, the equivalent voltage is calculated from summing the produced voltage in each individual coil for DLDCG. The same procedure is applied for DLSRG, coils 1,2,3,4 from 1st layer, and coils 5,6,7,8 from 2nd layer are in series and they belong to phase A.

The terminal voltage belonging to phase A under different loads are calculated in appropriate switching cycle and presented in Fig. 8 and Fig. 9 for dc and reluctance generators, respectively.

In these figures, the produced voltages in negative and positive period are clearly shown. It is worth mentioning here that, the stator and rotor cores are made of a non-oriented silicon steel lamination. The magnetization curve is taken from manufacturer's data sheet for M-27 steel.

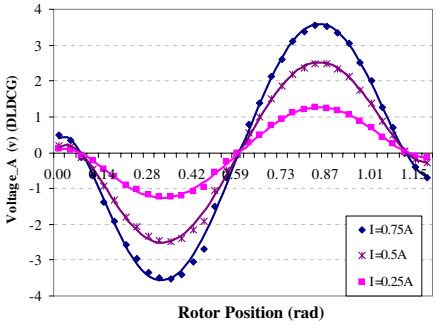

Figure 8. The terminal voltage for phase A in DLDCG.

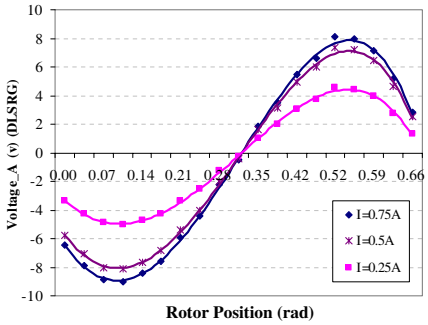

Figure 9. The terminal voltage for phase A in DLSRG.

As seen from Fig. 8 the maximum amplitude of generated voltage in DLDCG is 1.25, 2.5 and 3.5 volt under field currents of 0.25, 0.5 and 0.75 (A), respectively. On the other side, it is shown that, the magnitude of produced voltage in phase A has 2 and 3 times higher value when the field current has increased by factors of 2 and 3. It means the percentage of increasing output voltage is proportional to percentage variation of filed current (Eq. (3)).

$$\Delta V = \Delta I_f \tag{3}$$

Figure 9 shows the generated voltage waveform in DLSR generator that has its maximum value at 4.5, 7.3 and 8.1 volts under different mentioned field currents, respectively. The test condition for this machine is similar to the dc generator. Moreover, it is observed that the amount of produced voltage in phase A has 1.63 and 1.8 times higher values when the field current has increased by factors of 2 and 3. On other hands, the percentage of increasing in output voltage is not proportional to percentage variation of filed current such as the dc machine. It has linear relation that can be expressed in the form of:

$$\Delta V = 0.1739\Delta I_f + 1.2869 \tag{4}$$

Consequently, it can be concluded that the achieved terminal voltage in reluctance generator is higher than that of the dc generator under different loadings for the same conditions.

One of the major factors in obtaining different generated voltage between the two generator models is due to the different number of poles participating in voltage production. In SR generator eight poles and in DC generator six poles are joined to produce output voltage in one phase.

5. EXPERIMENTAL VERIFICATION

The proposed generators have been fabricated and tested for performance and functionality in the laboratory. Fig. 10 illustrates the novel brushless dc and switched reluctance generators fabricated in the laboratory.

The terminal voltage of the generators was obtained by the help of a prime mover to turn the generator shaft at a constant speed.

The generated voltage for a field current of 0.5 A was measured. The actual output voltages for two consecutive phases are also shown in Fig. 11.

It was observed that the terminal voltage shows lower value than computed which is expected (about 19%–24%), since, the silicon sheet steel material used to build the generators is not quite what is used for the numerical analysis.

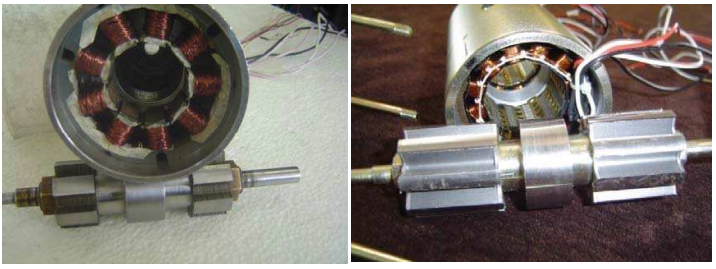

(a) (b)

Figure 10. The actual generators; (a) DLDC, (b) DLSR.

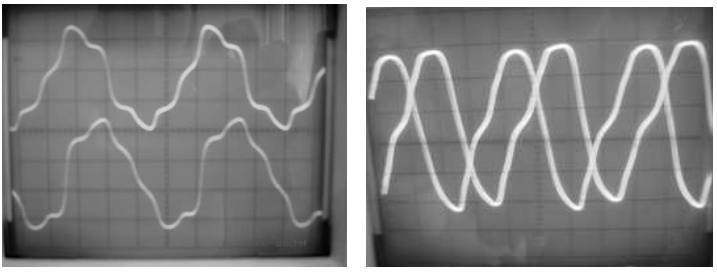

(a) 1 volt/div (b) 2 volt/div

Figure 11. Output voltages for two consecutive phases from; (a) DLDC, (b) DLSR generators.

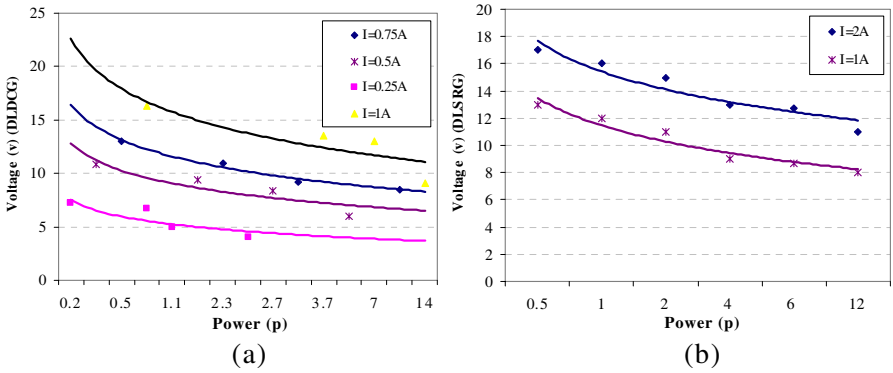

Figure 12. Output voltage vs. power (2500 rpm) from; (a) DLDC, (b) DLSR generators.

Figure 11(a) clearly shows the harmonics in dc generator output voltage which is due to slot harmonics as well as saturation in the rotor/stator poles. Fig. 11(b) depicts saturation in the SRG output voltage.

The speed of the motor is kept at 2500 rpm under different loads for various field currents. The output power versus the rectified output voltage is measured. The results of these tests are shown in Figs. 12(a), (b) for DLDC and DLSR generators respectively. The power curve fitting has been used for the data points.

6. CONCLUSION

In this paper, two new generator units were tested numerically and experimentally and then some of the generator parameters are obtained and compared. The experimental output voltage for SRG shows clearly the effect of saturation on the waveform which has a high content of third harmonics while the Brushless dc shows more tooth harmonics due to variation of the airgap. The average power obtained from the brushless dc generator for the same amount of field current magnitude is 10% higher than that of SRG. Comparing the plots of output voltage waveforms developed by the generator units, it can be seen that the DLDCG show about 50% higher voltages (in maximum value) than SRG. Since no permanent magnet is used in either of the generator units then they are very rugged and durable and have the potential to be used in very harsh environments. The output voltage magnitudes from the generator units are easily controlled by controlling the field current. The comparative study on the above two machines shows the

DLSR machine has better electromagnetic property and the DLDC machine has better mechanical behavior.

ACKNOWLEDGMENT

This work was supported by vice-presidency of research and technology of Shahid Beheshti University.

REFERENCES

1. Schofield, N. and S. Long, "Generator operation of a switched reluctance starter/generator at extended speeds," *IEEE Transactions on Vehicular Technology*, Vol. 58, No. 1, 48–56, 2009.
2. Lee, H., et al., "Practical control for improving power density and efficiency of the BLDC generator," *IEEE Transactions on Power Electronics*, Vol. 20, No. 1, 192–199, 2005.
3. Lee, H. W., T. H. Kim, and M. Ehsani, "Maximum power throughput in the multiphase brushless DC generator," *IEE Proceedings Electric Power Applications*, Vol. 152, No. 3, 501–508, 2005.
4. Kim, T., H. W. Lee, and M. Ehsani, "Position sensorless brushless DC motor/generator drives: Review and future trends," *IET Electric Power Applications*, Vol. 1, No. 4, 557–564, 2007.
5. Chen, H. C., T. Y. Tsai, and C. K. Huang, "Low-speed performance comparisons of back-EMF detection circuits with position-dependent load torque," *IET Electric Power Applications*, Vol. 3, No. 2, 160–169, 2009.
6. Zhang, Z., Y. Yan, S. Yang, et al., "Development of a new permanent-magnet BLDC generator using 12-phase half-wave rectifier," *IEEE Transactions on Industrial Electronics*, Vol. 56, No. 6, 2023–2029, 2009.
7. Chen, H. and J. J. Gu, "Implementation of the three-phase switched reluctance machine system for motors and generators," *IEEE Transactions on Mechatronics*, Vol. 15, No. 3, 421–432, 2010.
8. Torkaman, H. and E. Afjei, "FEM analysis of angular misalignment fault in SRM magnetostatic characteristics," *Progress In Electromagnetics Research*, Vol. 104, 31–48, 2010.
9. Afjei, E., A. Seyadatan, and H. Torkaman, "A new two phase bidirectional hybrid switched reluctance motor/field-assisted generator," *Journal of Applied Sciences*, Vol. 9, No. 4, 765–770, 2009.

10. Ding, W. and D. Liang, "Dynamic modeling and control for a switched reluctance starter/generator system," *International Conference on Electrical Machines and Systems*, 3315–3320, 2008.
11. Ferreira, C. A., S. R. Jones, W. S. Heglund, et al., "Detailed design of a 30-kW switched reluctance starter/generator system for a gas turbine engine application," *IEEE Transactions on Industry Applications*, Vol. 31, No. 3, 553–561, 1995.
12. Echenique, E., J. Dixon, R. Cardenas, et al., "Sensorless control for a switched reluctance wind generator, based on current slopes and neural networks," *IEEE Transaction on Industrial Electronics*, Vol. 56, No. 3, 817–825, 2009.
13. Cardenas, R., R. Pena, M. Perez, et al., "Control of a switched reluctance generator for variable-speed wind energy applications," *IEEE Transaction on Energy Conversion*, Vol. 20, No. 4, 781–791, 2005.
14. Fahimi, B., A. Emadi, and R. B. Sepe, Jr., "A switched reluctance machine-based starter/alternator for more electric cars," *IEEE Transactions on Energy Conversion*, Vol. 19, No. 1, 116–124, 2004.
15. Afjei, E. and H. Torkaman, "The novel two phase field-assisted hybrid SRG: Magnetio static field analysis, simulation, and experimental confirmation," *Progress In Electromagnetics Research B*, Vol. 18, 25–42, 2009.
16. Hanselman, D. C., *Brushless Permanent Magnet Motor Design*, McGraw-Hill, New York, 1994.
17. Afjei, E. and H. Toliyat, "A novel hybrid brushless dc motor/generator for hybrid vehicles applications," *International Conference on Power Electronics, Drives and Energy Systems*, 1–6, 2006.
18. Ravaud, R., G. Lemarquand, V. Lemarquand, and C. Depollier, "The three exact components of the magnetic field created by a radially magnetized tile permanent magnet," *Progress In Electromagnetics Research*, Vol. 88, 307–319, 2008.
19. Ravaud, R., G. Lemarquand, V. Lemarquand, S. I. Babic, and C. Akyel, "Mutual inductance and force exerted between thick coils," *Progress In Electromagnetics Research*, Vol. 102, 367–380, 2010.
20. Ravaud, R., G. Lemarquand, V. Lemarquand, S. Babic, and C. Akyel, "Mutual inductance and force exerted between thick coils," *Progress In Electromagnetics Research*, Vol. 102, 367–380, 2010.
21. Torkaman, H. and E. Afjei, "Magnetio static field analysis

regarding the effects of dynamic eccentricity in switched reluctance motor," *Progress In Electromagnetics Research M*, Vol. 8, 163–180, 2009.

22. Torkaman, H. and E. Afjei, "Hybrid method of obtaining degrees of freedom for radial airgap length in SRM under normal and faulty conditions based on magnetiostatic model," *Progress In Electromagnetics Research*, Vol. 100, 37–54, 2010.
23. Magnet CAD package, *User Manual*, Infolytica Corporation Ltd., 2007.